DOI: 10.1002/asia.201403205

CHEMISTRY
AN ASIAN JOURNAL
Full Paper

Gels

Charge Transfer Induces Formation of Stimuli-Responsive, Chiral, Cohesive Vesicles-on-a-String that Eventually Turn into a Hydrogel

Subham Bhattacharjee[a] and Santanu Bhattacharya*[a, b]

Abstract: A charge transfer (CT) mediated two-component, multistimuli responsive supergelation involving a L-histidine-appended pyrenyl derivative (PyHisOMe) as a donor and an asymmetric bolaamphiphilic naphthalene-diimide (Asym-NDI) derivative as an acceptor in a 2:1 mixture of H_2O/MeOH was investigated. Asym-NDI alone self-assembled into pH-responsive vesicular nanostructures in water. Excellent selectivity in CT gel formation was achieved in terms of choosing amino acid appended pyrenyl donor scaffolds. Circular dichroism and morphological studies suggested formation of chiral, interconnected vesicular assemblies resembling "pearls-on-a-string" from these CT mixed stacks. XRD studies revealed the formation of monolayer lipid membranes from these CT mixed stacks that eventually led to the formation of individual vesicles. Strong cohesive forces among the interconnected vesicles originate from the protrusion of the oxyethylene chains from the surfaces of the chiral vesicles.

Introduction

Charge-transfer (CT) crystals comprising alternately/cofacially arranged donor and acceptor aromatic molecular scaffolds are interesting, as they have excellent conducting properties.[1a] Metallic conductivity of CT crystals comprising tetrathiafulvalene and 7,7,8,8-tetracyanoquinodimethane was reported nearly three decades ago.[1a] Thereafter, several other reports emphasized the utilization of CT interaction in superconductivity, semiconductivity, and ferroelectricity.[1b,c] However, research work to construct CT-mediated two-component assemblies,[2] especially gels,[3] has been performed only relatively recently. Naphthalene-diimide (NDI) derivatives, some of the most promising n-type organic semiconductors, may be used as acceptors for suitable donor scaffolds to fabricate such CT-induced assemblies.[3e,f] Recently, Ghosh and co-workers reported CT-mediated assemblies by using NDI moiety as an acceptor and pyrene as a donor.[2c,d]

Supramolecular chirality can be regarded as an expression of absolute molecular chirality in macromolecular form. Nature has the amazing ability to construct helical assemblies that span from nanoscopic to macroscopic dimensions, together with giant superstructures, by using intriguing spatiotemporal programming language and elegant architectural plans. Inspired by nature, various divergent reversible, noncovalent, weak interactions including mostly H-bonding forces have been utilized to fabricate a number of artificial assemblies with preferential handedness.[4] In particular, the gelation-triggered construction of helical architectures[5] from chiral or even achiral molecular building blocks has drawn immense attention recently.

On the other hand, most supramolecular gels with a divergent class of molecular scaffolds are formed through the entanglement of fibrillar networks; in contrast, a particularly intriguing class of gels, especially hydrogels, is vesicular gels.[6] The individual vesicles that may be considered as "monomers" undergo fusion or come in close contact with each other through intervesicular cohesive forces to develop vesicle strings resembling apparent polymerization of the sole vesicles that macroscopically eventually act as a viscoelastic gel. Vesicle gels are also promising in the sense that they have potential applications in the field of medicinal chemistry, including drug delivery and tissue engineering.[7]

Two-component gels are fundamentally different from single-component ones, at least in terms of the design strategy. Two-component gels can be formed through metal-ion coordination,[8] H-bonding or halogen-bonding interactions,[9] donor–acceptor type interactions,[3] acid–base (salt-type) interactions,[10] and so forth. The design of two-component gels requires a more clever approach than that required for single-component gels, because the structure, mechanical, optical, and other properties of two-component gels can be conveniently tuned and considerably improved simply by changing the molar ratio of the components.[10e] In the present work, we demonstrate the remarkable role of CT, which assists in two-

---

[a] S. Bhattacharjee, Prof. Dr. S. Bhattacharya
Department of Organic Chemistry
Indian Institute of Science
Bangalore 560012, Karnataka (India)
Fax: (+91) 80-23600529
E-mail: sb@orgchem.iisc.ernet.in

[b] Prof. Dr. S. Bhattacharya
Honorary Professor
Jawaharlal Nehru Centre for Advanced Scientific Research
Bangalore 560064, Jakkur (India)

Supporting Information for this article is available on the WWW under http://dx.doi.org/10.1002/asia.201403205.

© 2015 Wiley-VCH Verlag GmbH & Co. KGaA, Weinheim

component supramolecular gelation. The first phase of our investigation focused on the self-assembly properties of a novel asymmetric bolaamphiphilic NDI derivative (Asym-NDI). Interestingly, Asym-NDI self-assembles in water to generate pH-responsive vesicular assemblies, and this has been proven through dye encapsulation along with various microscopic studies. Then, we investigated CT gelation between a L-histidine-appended pyrenyl derivative (PyHisOMe) as a donor and Asym-NDI as an acceptor. Excellent selectivity in gel formation was also achieved in terms of the choice of the amino acid termini in the pyrenyl donors. Detailed investigations clearly suggest the formation of chiral interconnected vesicles resembling "pearls-on-a-string" in the nanoscale dimension, whereas they macroscopically form hydrogels through intertwining of the vesicle strings. Intermolecular H-bonding interactions among the hydrazide groups of Asym-NDI play a crucial role in assisting the CT interactions. Moreover, the hydrogel also responds to a variety of stimuli and undergo reversible sol–gel transition upon removal of the stimuli. To the best of our knowledge, this is the first report of CT-induced supramolecular gels with "vesicles-on-a-string" morphology that show excellent selectivity in gelation, supramolecular chirality, and multistimuli responsiveness.

Results and Discussion

Synthesis

The syntheses of PyHisOMe, PyPheOMe, PyTrpOMe, and PyPhe-COOH were performed by using standard peptide coupling reagents, and these compounds were characterized by ^{1}H NMR, ^{13}C NMR, and FTIR spectroscopy; ESI-MS; and elemental analyses (Scheme 1 and the Supporting Information). The Asym-NDI derivative was synthesized by heating an equimolar mixture of 1,4,5,8-naphthalenetetracarboxylic dianhydride, isoniazide, and 3,4,5-tris{2-[2-(2-methoxyethoxy)ethoxy]ethoxy}benzohydrazide in DMF at reflux under an inert atmosphere for 12 h. The crude product was purified by silica gel column chromatography (3–4% MeOH/$CHCl_3$; see Scheme 1 and the Supporting Information).

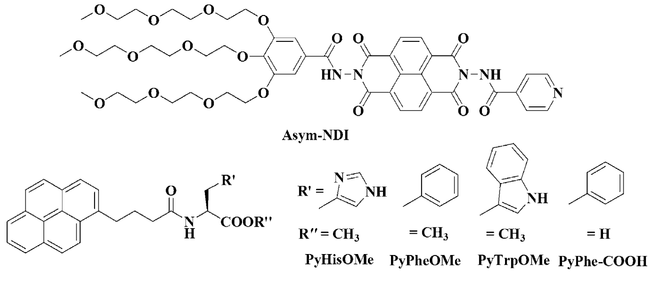

Scheme 1. a, b) Molecular structures of the acceptor (Asym-NDI) and various amino acid appended pyrenyl donors used in this investigation.

Self-assembly studies of Asym-NDI

Examination of bolaamphiphilic Asym-NDI (50 μM) in MeOH, in which it molecularly dissolves, by UV/Vis spectroscopy revealed well-resolved absorption bands at $\lambda = 355$ and 375 nm with vibronic features (Figure 1 a). In contrast, in water both absorption bands were redshifted to $\lambda = 357$ and 381 nm, respectively, with concomitant decreases in the intensities of the bands. In addition, the UV/Vis absorption spectrum in water displayed significant scattering in the $\lambda = 400$–550 nm range, which suggests aggregation-induced loss of transparency of the solution in water even at a concentration of 50 μM (Figure 1 f). Concentration-dependent UV/Vis studies of Asym-NDI were performed in an attempt to determine the critical aggregation concentration in water (Figure S1 a, Supporting Information). However, the critical concentration leading to aggregation could not be determined precisely from the concentration dependence of the absorbance at $\lambda = 380$ nm.

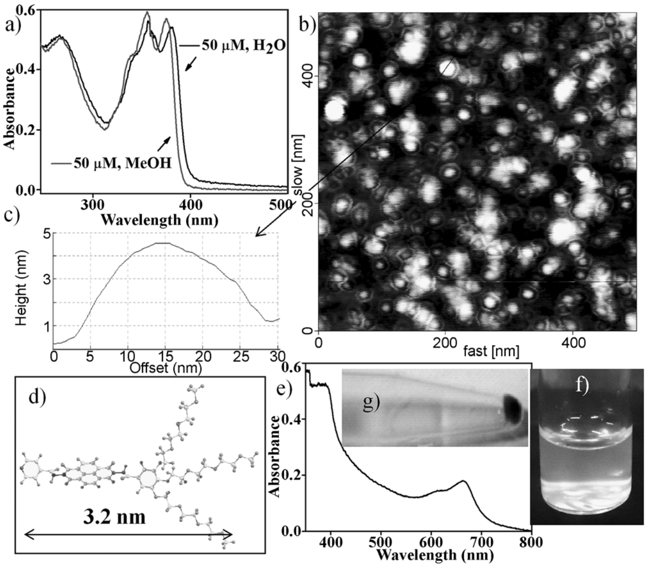

Figure 1. a) UV/Vis absorption spectra of Asym-NDI in MeOH and H_2O, [Asym-NDI] = 50 μM. b) AFM image of Asym-NDI (50 μM) and c) height image of a single vesicle. d) Energy-minimized structure of Asym-NDI. e) Absorption spectrum of the encapsulated dye in the vesicular compartment of Asym-NDI. f, g) Photographs of a suspension of Asym-NDI (1 mg mL^{-1}) in water and precipitates of the vesicular aggregates along with encapsulated dye.

Dynamic light scattering (DLS) experiments were performed to unambiguously confirm the existence of aggregates in solution ([Asym-NDI] = 50 μM), and these experiments revealed an average hydrodynamic diameter (D_h) of the aggregates of (76 ± 1) nm (Figure S1 b). To investigate the nature of the supramolecular assemblies, atomic force microscopy (AFM) studies were performed by using a suspension of Asym-NDI (50 μM). The AFM images in Figure 1 b show the presence of dense spherical disc-like aggregates with an average diameter of approximately 25–35 nm and a height of approximately 4.5 nm (Figures 1 b, c and S2 a, b). The smaller size of the aggregates observed under AFM relative to that observed by DLS may be attributed to shrinkage of the aggregates during solvent evaporation.[11] The diameter of Asym-NDI along the long molecular axis, as determined by energy minimization of the molecule by using B3LYP/6-31G* level computations, was approximately 3.2 nm (Figure 1 d). Thus, the size of a single Asym-NDI molecule is considerably smaller than the diameter of the aggregates observed under AFM and DLS; this indicates the vesicle-like nature of the aggregates.[11] Similar spherical aggregates resembling vesicles were also observed under transmission electron microscopy (TEM) investigations of a suspension of Asym-NDI (50 μM; Figure S2 c,d). XRD studies of cast aggregates of Asym-NDI showed the presence of three well-resolved Bragg reflections at $2\theta = 2.59$ (3.4 nm), 5.2 (1.7 nm) and 7.91 (1.12 nm) in the low-angle region with a spacing ratio of 1:1/2:1/3 (Figure S2 c). Thus, the presence of regularly sharp XRD peaks suggest lamellar arrangement of Asym-NDI with a periodicity of approximately 3.4 nm, which is slightly larger than the molecular diameter (3.2 nm); this is indicative of the formation of monolayer lipid membranes (MLMs).[12] These MLMs, in turn, develop vesicular nanoassemblies through rolling-up, as evidenced from their turbid texture as an aqueous suspension (Figure 1 f). Interestingly, the turbid suspension transformed into a clear solution at pH 2 owing to protonation of the pyridyl end group of Asym-NDI, which is indicative of dissolution of the vesicular aggregates (Figure S3 a).

Sedimentation experiments were performed to gain further evidence of vesicle formation. In particular, the encapsulation ability of the vesicular aqueous solution of Asym-NDI (Figure 1 f) was checked by using a hydrophilic dye, that is, methylene blue (MB).[11] A mixture of Asym-NDI (1 mg) and MB (0.1 mg) in water (1 mL) was sonicated for approximately 15 min, and the resultant suspension was centrifuged, which allowed precipitation of the encapsulated vesicular aggregates. The supernatant was carefully removed, and the precipitate was redispersed in water (1 mL); the same procedure was repeated twice to remove the un-encapsulated dye, if any. Interestingly, the precipitate thus obtained retained its significantly dark-blue color, which suggests encapsulation of the dye inside the vesicular aggregates (Figure 1 g). The precipitate thus obtained was resuspended in water (1 mL), and the UV/Vis spectrum of this suspension showed an absorption band at $\lambda = 664$ nm (Figure 1 e). This band is due to the entrapped MB dye and further confirms its encapsulation with an encapsulation efficiency of 2.2 % (Figure S3 b); it also confirms the existence of an inner aqueous compartment within the vesicular aggregates. Poor encapsulation efficiency may be attributed to the smaller size of the vesicles and hence the vesicular core.

Charge-transfer-interaction triggered hydrogelation

Wilson et al. examined the CT interactions among nine combinations of electron-rich donors and electron-poor acceptors by using various spectroscopic techniques. These studies revealed high association constants between pyrene and the NDI derivatives.[13] In the present report, various amino acid appended pyrenyl derivatives were prepared as possible donor scaffolds against the above-mentioned NDI derivative. Interestingly, Asym-NDI was able to form CT complexes with all of the above pyrenyl derivatives in MeOH. The CT interaction was initially evident from naked-eye detection of the deep violet color (resulting from the formation of a CT complex) of the MeOH solution.

However, aggregation of the CT complex was not observed in MeOH alone. To introduce solvophobic interactions among the CT complexes, water was gradually added to the preformed MeOH solution of the CT complex. More specifically, addition of water to a MeOH solution (in a proportion of 2:1 *v*/*v* H_2O/MeOH) of the PyHisOMe/Asym-NDI = 1:1 CT complex at a PyHisOMe concentration of 2.4 mM caused immediate aggregation, which eventually produced a translucent gel after ageing for approximately 10–12 min (Figure 2). Interestingly, the 1:1 CT complex formed a gel at a concentration as low as 0.84 mM, and this demonstrates an encapsulation of more than 44 000 water molecules and almost 10 000 methanol molecules by a single CT unit. Thus, the present hydrogel belongs to the category of supergelators.[14] Surprisingly, neither the mixture of PyPheOMe (or PyTrpOMe)/Asym-NDI = 1:1 produced a gel if water was added to the MeOH solution (H_2O/MeOH = 1:2) of the mixture; instead, only precipitation was observed. The gelation propensity of PyPheCOOH with Asym-NDI (1:1 molar ratio) was also checked by slowly adding water to the MeOH solution of the mixture. However, in this instance gelation was also not observed, although PyPheCOOH has one free −COOH group that may participate in intermolecular H-bonding. Thus, remarkable selectivity in the formation of the gel in terms of the choice of the amino acid termini in the pyrenyl donor was observed. Moreover, the selective gelation of the PyHisOMe/Asym-NDI = 1:1 CT complex in a 2:1 mixture of H_2O/MeOH also suggests that the L-histidine unit has a significant role in forming intermolecular H-bonds in addition to the intermolecular H-bonding mediated by the amide units.

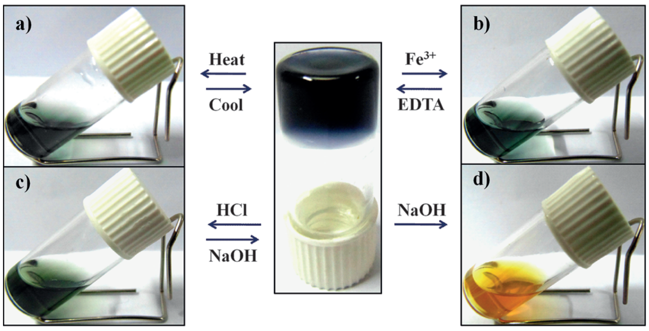

Figure 2. The gel–sol transitions of the PyHisOMe/Asym-NDI = 1:1 CT hydrogel triggered by a variety of stimuli (heat/cold, acid/base, Fe^{+3}/EDTA), [PyHisOMe] = 2.4 mM in a 2:1 mixture of H_2O/MeOH.

Supramolecular gels often respond to a variety of external stimuli such as heat, light, metal ions, pH, salts, ultrasound, and agitation, and they often revert back to the gel state with concomitant removal of the stimuli.[15] With this in mind, we also investigated the possible consequences of exposing the present 1:1 CT gel to various stimuli. The CT gel showed thermoreversibility (Figure 2a). Recently, Liu and co-workers demonstrated the hydrogelation of L-histidine-based bolaamphiphiles by using the metal-ion coordination ability of the imidazole N atom of the L-histidine unit.[12] To examine the impact of the present gel system in the presence of metal ions, we added Fe^{3+} to the preformed gel (PyHisOMe/Fe^{3+} = 1:1). This caused immediate dissolution of the gel state to produce an intense greenish-colored sol (Figure 2b). The intense greenish color of the sol indicates that the CT interactions between the donor and acceptor pairs remain unaffected by metal-ion coordination of the L-histidine unit of the gelators. Reformation of the gel state was realized just by adding a small excess amount of ethylenediaminetetraacetic acid disodium salt (EDTA; Fe^{3+}/EDTA = 1:1.5); EDTA binds preferentially to the metal ion, which frees the gelators. It is also well known that the basic nitrogen atom of the L-histidine unit can be protonated easily. The pyridyl N atom of Asym-NDI is also pH sensitive. Thus, the preformed gel was treated with a few drops of 2 N HCl solution. As a result, the 1:1 CT gel immediately turned into a sol (pH 2) but still kept the CT interactions intact, as revealed by retention of its violet color (Figure 2c). However, gelation was realized if the added acid was neutralized by 2 N NaOH. Similarly, the addition of a few drops of 2 N NaOH onto the top of a preformed gel also led to the disruption of the gel network along with abolition of the CT interactions (Figure 2d). Given that the hydrazide group of Asym-NDI is significantly acidic, the addition of a strong base presumably leads to deprotonation of the hydrazide group, which plays a significant role in H-bonding-assisted enhanced CT interactions among the donor–acceptor pairs. Thus, the deprotonation of the hydrazide group resulted in weakening of the CT interactions.

Titration of PyHisOMe (1 mM) in MeOH with increasing amounts of Asym-NDI was performed under UV/Vis spectroscopy (Figure 3a). Notably, the CT band remained very weak even at a 1:1 molar ratio of the CT complex. This suggests that the CT interactions among the donor–acceptor pairs are presumably negligible in MeOH, which results in failure to form an effective gel in MeOH alone. Concentration-dependent absorption spectra of the 1:1 CT complex in a 2:1 mixture of H_2O/MeOH, however, showed the presence of a strong CT band, which gradually disappeared with a concomitant decrease in the concentration of the gelators (Figure 3b). The association constant (K) of the 1:1 CT complex was determined to be approximately $0.9\times10^3\,M^{-1}$ (Figure S4).[3e] Temperature-dependent UV/Vis studies of the 1:1 CT complex (PyHisOMe = 1.7 mM) were also performed. These revealed that the CT band was still present in the heated sol and that the intensity of the CT band gradually increased by decreasing the temperature to 25 °C, which suggests aggregation-triggered enhancement in the CT interactions (Figure 3c). UV/Vis studies were also performed with the 1:1 CT complex at various compositions of H_2O/MeOH to determine the "critical" composition of the solvents necessary for aggregation (Figure 3d). Interestingly, the 1:1 CT complex (PyHisOMe = 0.25 mM) showed an almost negligible CT band in the absorption spectrum in MeOH alone. The CT band centered at $\lambda = 575$ nm gradually appeared with a concomitant increase in the proportion of water and suddenly increased up to a significant extent in a 4:1 mixture of H_2O/MeOH, which suggests manifestation of the aggregation-induced enhanced CT interactions (Figure 3d, e). Notably, although the CT band at [PyHisOMe] = 0.25 mM was negligible in the 2:1 mixture of H_2O/MeOH (optimum solvent composition for gel formation), a significant enhancement in the CT intensity was observed in the 4:1 mixture of H_2O/MeOH, which suggests that the CT interactions were dependent on both the concentration of the gelator and the solvent composition.

The concentration-dependent fluorescence spectra of the 1:1 CT complex (Figure S5a) displayed emission in the range of

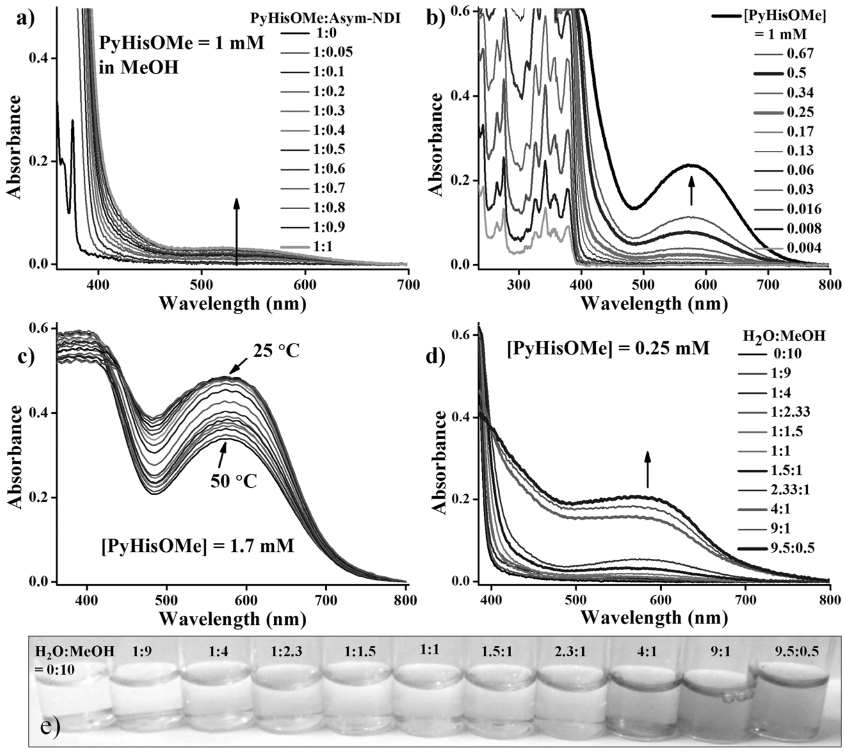

Figure 3. a) Titration of PyHisOMe in MeOH with increasing amounts of Asym-NDI under UV/Vis spectroscopy. b) Concentration-dependent UV/Vis spectra of the 1:1 CT complex in a 2:1 mixture of H_2O/MeOH. c) Temperature-dependent UV/Vis spectroscopy of the 1:1 CT complex in a 2:1 mixture of H_2O/MeOH; [PyHisOMe] = 1.7 mM. d) UV/Vis spectroscopy of the 1:1 CT complex at various compositions of H_2O/MeOH and e) photographs of the corresponding suspensions under normal light, [PyHisOMe] = 0.25 mM.

© 2015 Wiley-VCH Verlag GmbH & Co. KGaA, Weinheim

$\lambda = 350$ to 450 nm and slowly increased with a concomitant decrease in the gelator concentration and showed a maximum emission at a PyHisOMe concentration of 16 µM. The emission intensity further diminished with a decrease in the concentration. However, the excimer emission of PyHisOMe, characteristic for an aggregated PyHisOMe species, was not observed for any of the concentrations, and this indicates formation of a mixed stack donor–acceptor complex.[3a]

Because the CT gel is optically translucent in nature (Figure S5 b), it also provides an opportunity to investigate the aggregation properties in solution through time-dependent circular dichroism (CD) spectroscopy near or above the critical gelator concentration. For this experiment, an appropriate amount of water was added to the preformed solution of the 1:1 CT complex in MeOH ([PyHisOMe] = 2 mM, 2:1 H_2O/MeOH), and the resulting solution was immediately mixed thoroughly by mechanical agitation. The resultant solution was poured into a 1 mm cuvette as fast as possible and the CD signals were recorded with progressive aging of the solution. Interestingly, the solution did not display any CD signal after 1 min, which indicates that 1 min is not long enough to induce efficient helical supramolecular polymerization (Figure 4 a). A very weak bisignate negative CD signal started to evolve only after approximately 4 min, and this is indicative of detectable nucleation of chiral supramolecular polymerization at this time. After that, the CD intensity gradually increased to a significant extent with further aging of the solution, and the process started to saturate after approximately 30 min, which thus demonstrated gradual evolution of the left-handed helical (*M*-helical) aggregates from the isotropic state.[16] The intense bisignate negative Cotton signal that evolved over 30 min intersected the $\theta = 0^\circ$ line with an isodichroic point at $\lambda = 409$ nm. The bisignate Cotton signal displayed a maximum negative band at $\lambda = 555$ nm; this coincides with the absorption position of the CT band in the UV/Vis spectra and a maximum positive band at $\lambda = 355$ nm, which happens to be close to the λ_{max} of the pyrenyl unit of the 1:1 CT complex in the UV/Vis spectrum. A strong negative Cotton effect in the region of the CT band also suggests the induction of molecular chirality of PyHisOMe to the 1:1 CT complex at the supramolecular level. A plot of the CD intensity at $\lambda = 354$ nm versus time afforded a sigmoidal curve, which indicates the rate of helical supramolecular polymerization increased significantly after approximately 8 min and reached saturation after approximately 30 min (Figure 4 a, inset).

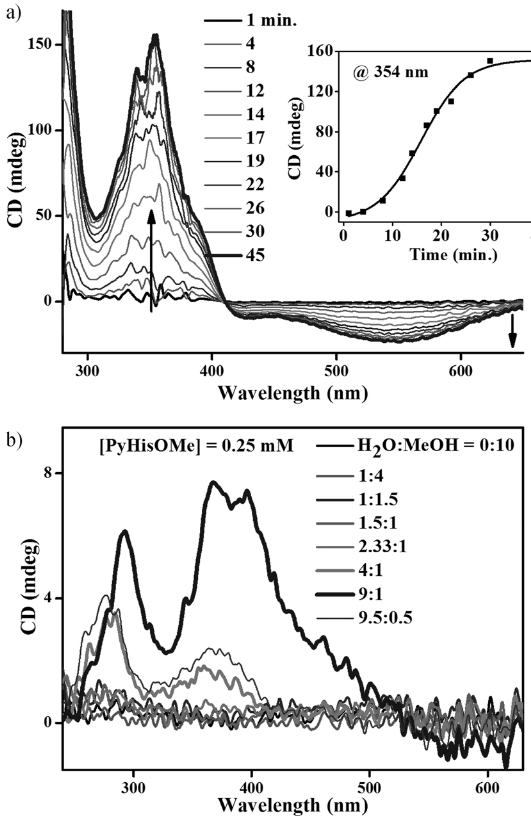

Figure 4. a) Evolution of the CD intensity upon aging a mixture of the 1:1 CT complex in a 2:1 mixture of H_2O/MeOH, [PyHisOMe] = 2 mM. Inset shows the plot of the CD intensity at $\lambda = 354$ nm versus time. b) CD spectra of the 1:1 CT complex at different compositions of H_2O and MeOH, [PyHisOMe] = 0.25 mM.

To verify the existence of supramolecular chirality originating from the molecular chirality of PyHisOMe, the temperature-dependent CD spectra of the 1:1 CT complex were recorded (Figure S5 c). A solution of the 1:1 CT complex ([PyHisOMe] = 2 mM) exhibited an intense bisignate negative Cotton signal at 25 °C. The intensive bisignate negative Cotton signal, however, slowly lost intensity with a gradual increase in the temperature and finally became CD silent at a temperature of approximately 50 °C, which is indicative of an apparent breakdown in the left-handed helical aggregates.

The CD spectra of the 1:1 CT complex were also recorded at variable compositions of MeOH and H_2O at a PyHisOMe concentration of 0.25 mM to affirm the growth of the left-handed assemblies beyond the "critical" solvent composition (Figure 4 b). Interestingly, in MeOH alone, the CD signal was almost silent, which indicates that the aggregation of the CT mixed stacks in MeOH alone is negligible. The CD signal, however, appeared with an increasing amount of water in MeOH in the proportion of H_2O/MeOH = 4:1. A relatively stronger bisignate negative Cotton effect was observed in a 9:1 mixture of H_2O/MeOH; this indicates an aggregation-induced enhancement in the CD signal and the formation of left-handed helical assemblies by the CT mixed stacks in this solvent composition. Notably, the critical solvent composition for the aggregation of the gelators at a PyHisOMe concentration of 0.25 mM was H_2O/MeOH = 4:1, although the gelator at a relatively high concentration (PyHisOMe = 2 mM) self-assembled in a 2:1 mixture of H_2O/MeOH to a "stable" gel state. Thus, the self-assembly of the gelators was not only dependent on the concentration but also on the composition of the solvents and temperature.

XRD studies of the xerogels of the 1:1 CT complex from a 2:1 mixture of H_2O/MeOH displayed one strong Bragg reflection in the low-angle regime at $2\theta = 2.59$ that corresponds to a repetitive distance of 3.4 nm of the layered structure (Figure 5 a). Given that the diameter of the layered structure was almost comparable to the extended length of the 1:1 CT complex ($\approx$3.2 nm; Figure 5 b), it is believed that the CT mixed

© 2015 Wiley-VCH Verlag GmbH & Co. KGaA, Weinheim

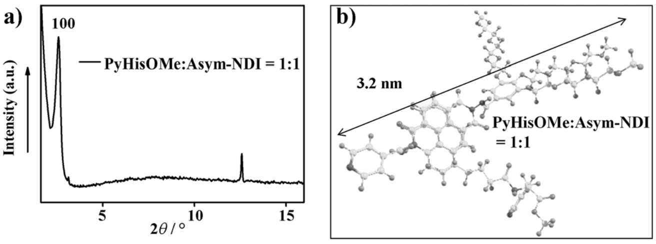

Figure 5. a) XRD studies of the 1:1 CT dried gel. b) An energy-minimized structure of the 1:1 CT complex.

stacks form MLMs through alternate self-assembly of the donor–acceptor pairs.[12] DLS studies of the solution of the 1:1 CT complex ([PyHisOMe] = 0.25 mM, H_2O/MeOH = 4:1) revealed the formation of aggregates with a D_h of (266 ± 19) nm, which suggests the existence of vesicular aggregates in solution (Figure S5 d).

Scanning electron microscopy (SEM) of the 1:1 CT gel at a PyHisOMe concentration of 0.25 mM from a 4:1 mixture of H_2O/MeOH confirmed the formation of vesicular aggregates with a diameter in the range of 80 to 230 nm, which are arranged in a "pearls-on-a-string" type fashion (Figure 6 a). Moreover, in some cases the individual vesicles remained "fused" together to form short fiber-like organizations in the nanoscale dimension (Figure 6 b). To verify the "pearls-on-a-string" type morphological features, AFM studies were also performed by using a solution of the gelators ([PyHisOMe] = 0.25 mM) from a 4:1 mixture of H_2O/MeOH. AFM analysis of a relatively large area of the mica surface evidenced the formation of entangled fiber-like networks (Figure 6 c). However, careful scanning of a smaller area of the mica surface revealed the formation of 1D fiber-like structures resulting from closely packed individual vesicles, and this led to the generation of the "pearls-on-a-string" type nanostructured pattern (Figures 6 d and S6 a, b). The formation of the fiber-like network through the closely packed linear arrangement of the vesicles unambiguously demonstrates that the vesicles are strongly cohesive in nature. Moreover, cluster-type aggregates were observed from a freeze-dried 1:1 CT gel above the critical gelator concentration (PyHisOMe = 2.4 mM; 2:1 H_2O/MeOH) under SEM, analysis of which indicated the formation of the former through fusion of the vesicular aggregates (Figure S6 c). This result also ruled out the possibility of evaporation-induced formation of vesicle strings. Menger et al. reported similar "vesicles-on-a-string" gels based on a series of gemini surfactants.[6a] Raghavan and co-workers very recently demonstrated the conversion of densely packed vesicle gels into helical microtubules as a function of time.[6d] Such equivalent morphological development such as micelle chaining resulting from kinetic self-assembly was also demonstrated by several groups.[17] In an attempt to determine the existence of the free vesicles, an AFM study was performed at a much lower concentration of the gelator ([PyHisOMe] = 0.05 mM). This showed the formation of free vesicular nanostructures with an average diameter of 90–200 nm and a height of 5–20 nm (Figure 6 e, f). Similar concentration-dependent morphological patterns were also observed by AFM in water (Figure S7).

The various rheological parameters of a soft material are extremely important in terms of the utility of the material in practical applications. Rheologically, gels are viscoelastic solid-like materials.[18] Oscillatory strain amplitude sweep experiments were performed with the 1:1 CT gels at three different concentrations (Figure 7 a). The G' value, that is, the viscoelastic character of the CT gel, progressively increased upon increasing the concentration of the gelator. Oscillatory frequency sweep experiments were also performed for the CT gel at various concentrations. The frequency sweep experiment showed that the G' value was always greater than the corresponding loss modulus, G'', value under an applied strain of 0.01 % in the angular frequency range of 1 to 100 rad s^{-1} and was also invariant to angular frequency. This suggests the viscoelastic nature of the CT gels over the entire angular frequency range (Figure S8).

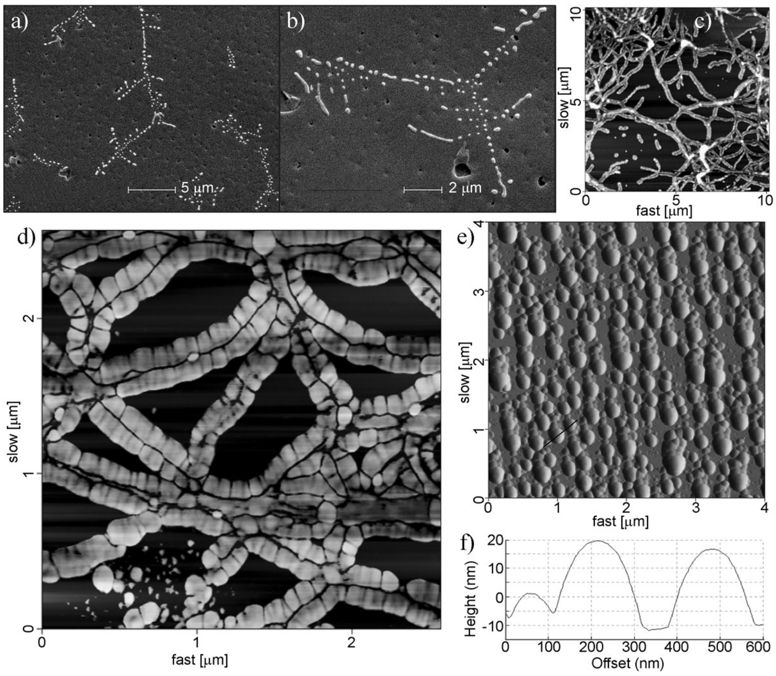

Figure 6. a, b) SEM and c, d) AFM images of the 1:1 CT system at different positions and magnifications, [PyHisOMe] = 0.25 mM. e, f) AFM image of the 1:1 CT system at [PyHisOMe] = 0.05 mM and the corresponding height image.

Progressive evolution of the 1:1 CT gel from the molecularly dissolved isotropic state was also realized from time-dependent

© 2015 Wiley-VCH Verlag GmbH & Co. KGaA, Weinheim

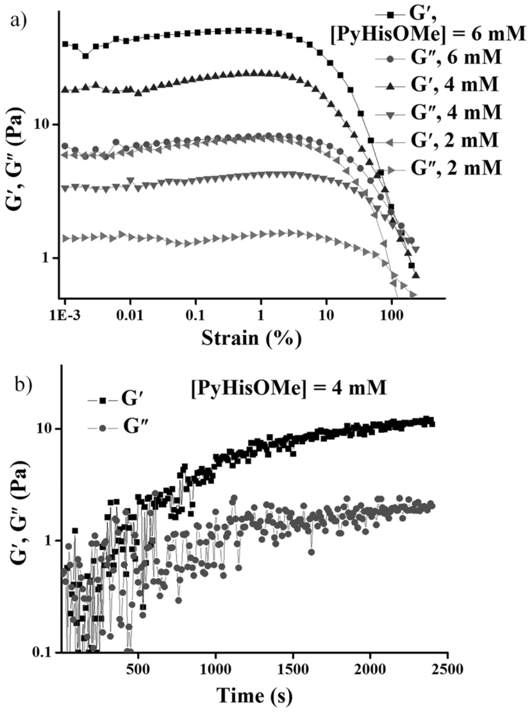

Figure 7. a) Amplitude–sweep rheology data of 1:1 CT gels in a 2:1 mixture of H_2O/MeOH at three different concentrations. b) Evolution of the viscoelastic gels from an apparently isotropic solution as a function of time, [PyHisOMe] = 4 mм.

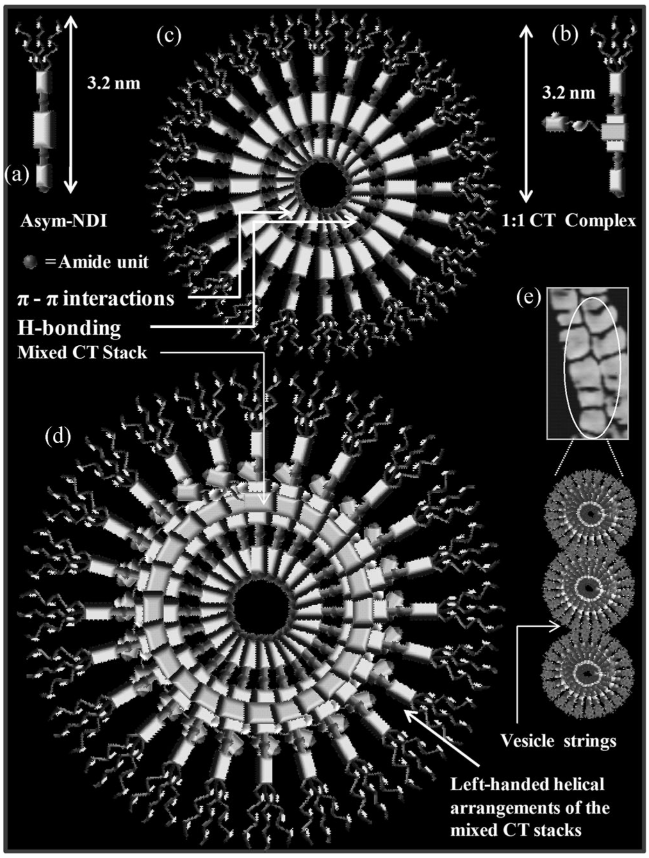

Figure 8. a, b) A cartoon representation of Asym-NDI and the 1:1 CT complex. c) Demonstration of the formation of vesicles of Asym-NDI in water through self-assembly of the MLMs; only the cross-section of the vesicle is shown for clarity. d) Demonstration of the formation of chiral vesicles from the left-handed helical arrangements of the mixed CT stacks in the MLMs; only the cross-section of the unilamellar vesicle is shown for clarity. e) Formation of "vesicles-on-a-string" through interdigitation of the oligo-oxyethylene chains.

measurement of the *G*′ and *G*″ values at an angular frequency of 6.28 rad s^{-1} and a strain of 0.01 % (Figure 7 b). Thus, to a solution of the 1:1 CT complex in MeOH, an appropriate amount of water was added at a time (H_2O/MeOH = 2:1). Subsequently, the resultant solution was mixed properly and placed on the rheometer as fast as possible. Initially, the *G*′ value was less than the respective *G*″ value, which was indicative of the solution state of the CT complex. Notably, the storage modulus *G*′ started to increase relative to the corresponding loss modulus *G*″, which suggested progressive evolution of the viscoelastic character upon aging of the solution. Thenceforth, the mechanical strength progressively increased and was almost saturated after 40 min; this confirmed robust gel formation from the isotropic solution state.

The larger size (diameter ≈90–200 nm) and height (≈5–20 nm) of the individual vesicles relative to the extended length of the 1:1 CT pairs indicates aggregation of the MLMs into multilayer structures in the vesicular wall. On the other hand, the supramolecular chirality was not reflected directly in the morphological features of the gelators. Thus, the combination of CD, XRD, and morphological studies clearly suggests that a left-handed helical arrangement of the mixed CT stacks in the vesicular walls leads to the formation of chiral vesicular aggregates (Figure 8 d). However, a closer look at the single 1:1 CT complex suggests that either side of the CT unit is considerably polar. The relative polarity of the two ends is significantly different owing to the asymmetric bolaamphiphilic nature of the CT unit. Given that the oligo-oxyethylene chains are more polar, they probably experience the hydrophilic H_2O/MeOH environment, and the relatively less polar pyridyl ends face the inner core of the individual vesicles. Thus, the surfaces of the vesicles are rich with polar oxyethylene chains, which may be attributed to the cohesive nature of the vesicles. The individual vesicles form a "pearls-on-a-string" or "fiber-like" assembly through interdigitation of the oxyethylene chains (Figure 8 e). The entanglement of the fiber-like structures creates 3D pockets, which are eventually filled up by the solvent molecules. Thus, the solvent molecules occupy the inner core of the vesicles as well as the 3D hydrophilic pockets that, in turn, cause gel formation. Notably, Asym-NDI did not form a coordination complex with any of the metal ions, including Ag^{+}, Cu^{2+}, and Zn^{2+}. It also remained in the unprotonated form even at pH 3. These observations suggest that the basicity of the pyridyl N atom of Asym-NDI is rather low, presumably as a result of the presence of the electron-withdrawing carbonyl group in the *para* position of the pyridine ring. Therefore, we did not consider H-bonding possibilities between the ʟ-histidine unit of PyHisOMe and the pyridine group of Asym-NDI during the CT-induced gelation process.

Conclusions

In conclusion, we explored the self-organization of novel asymmetric bolaamphiphilic naphthalene-diimide (Asym-NDI) into pH-responsive vesicles in water as the first phase of our investigations. However, in the second part, we demonstrated remarkable CT-mediated gelation of PyHisOMe/Asym-NDI = 1:1 charge-transfer (CT) mixed stacks in a 2:1 mixture of H_2O/MeOH. Aggregation of the CT stacks was not realized in MeOH alone; however, the addition of water to the methanol solution in a H_2O/MeOH ratio of 2:1 caused immediate aggregation and subsequent gel formation within a few minutes. UV/Vis spectral studies also confirmed that weak CT interactions among the donor–acceptor pairs in MeOH increases significantly in a 2:1 mixture of H_2O/MeOH owing to hydrophobic effects. The CT interactions are further assisted through intermolecular H-bonding interactions among the hydrazide units of Asym-NDI and are dependent on the concentration, temperature, and solvent composition. Unlike the PyHisOMe/Asym-NDI = 1:1 CT complex, the failure of PyPheOMe, PyTrpOMe, and PyPheCOOH to form gels with the acceptor, Asym-NDI, is noteworthy. This further suggests that the L-histidine unit of PyHisOMe has a crucial role in preventing precipitation of the aggregates from solution. This occurs through several H-bonding interactions of the histidine unit with the gelators as well as with the solvent molecules, and thereby selective gel formation occurs in a 2:1 mixture of H_2O/MeOH. The presence of supramolecular left-handed chiral assemblies was further evidenced from circular dichroism studies, although it was not directly apparent from the morphological features of the gels. Rather, interconnected vesicular assemblies arranged in a "pearls-on-a-string" fashion as a result of intervesicular cohesive forces were detected from the microscopic studies. The intervesicular cohesive force arises presumably from projection of the oligo-oxyethylene chains from the surface of the vesicles. The "vesicles-on-a-string" like morphology, in turn, produces a fiber-like intertwined network that eventually immobilizes the resulting mixture. XRD studies suggest the CT mixed stacks self-assemble in a left-handed helical fashion in the monolayer lipid membranes, and this eventually leads to the fabrication of the chiral vesicular architectures. In addition, multistimuli responsiveness of the CT gel was also demonstrated. In a nutshell, this is the first report of a supramolecular CT gel that possesses all of these features, including "vesicles-on-a-string" morphology. Accordingly, the present system may be useful in stimuli-responsive drug delivery or in materials-release applications.

Acknowledgements

This work was supported by J. C. Bose fellowship of Department of Science & Technology DST to S. Bhattacharya. S. Bhattacharjee thanks the Council of Scientific & Industrial Research (CSIR)

Keywords: charge transfer · helical structures · selectivity in supergelation · stimuli responsive · vesicle strings

[1] a) J. P. Ferraris, T. O. Poehler, A. N. Bloch, D. O. Cowan, *Tetrahedron Lett.* **1973**, *14*, 2553 – 2556; b) J. i. Yamada, H. Akutsu, *Chem. Rev.* **2004**, *104*, 5057 – 5083; c) S. K. Park, S. Varghese, J. H. Kim, S. O. Yoon, K. Kwon, B. K. An, J. Gierschner, S. Y. Park, *J. Am. Chem. Soc.* **2013**, *135*, 4757 – 4764.

[2] a) Y. Yamamoto, T. Fukushima, Y. Suna, N. Ishii, A. Saeki, S. Seki, S. Tagawa, M. Taniguchi, T. Kawai, T. Aida, *Science* **2006**, *314*, 1761 – 1764; b) C. Wang, Z. Wang, X. Zhang, *Acc. Chem. Res.* **2012**, *45*, 608 – 618; c) S. Ghosh, *Chem. Commun.* **2014**, *50*, 11657 – 11660; d) S. Ghosh, *Angew. Chem. Int. Ed.* **2014**, *53*, 1092 – 1097; *Angew. Chem.* **2014**, *126*, 1110 – 1115.

[3] a) U. Maitra, P. V. Kumar, N. Chandra, L. J. D'Souza, M. D. Prasanna, A. R. Raju, *Chem. Commun.* **1999**, 595 – 596; b) P. Babu, N. M. Sangeetha, P. Vijaykumar, U. Maitra, K. Rissanen, A. R. Raju, *Chem. Eur. J.* **2003**, *9*, 1922 – 1932; c) J. R. Moffat, D. K. Smith, *Chem. Commun.* **2008**, 2248 – 2250; d) K. V. Rao, K. Jayaramulu, T. K. Maji, S. J. George, *Angew. Chem. Int. Ed.* **2010**, *49*, 4218 – 4222; *Angew. Chem.* **2010**, *122*, 4314 – 4318; e) M. R. Molla, S. Ghosh, *Chem. Eur. J.* **2012**, *18*, 9860 – 9869; f) S. K. M. Nalluri, C. Berdugo, N. Javid, P. W. J. M. Frederix, R. V. Ulijn, *Angew. Chem. Int. Ed.* **2014**, *53*, 5882 – 5887; *Angew. Chem.* **2014**, *126*, 5992 – 5997; g) S. Basak, S. Bhattacharya, A. Datta, A. Banerjee, *Chem. Eur. J.* **2014**, *20*, 5721 – 5726; h) S. S. Babu, V. K. Praveen, A. Ajayaghosh, *Chem. Rev.* **2014**, *114*, 1973 – 2129.

[4] a) C. Xu, R. Liu, A. K. Mehta, R. C. G. -Ferreira, E. R. Wright, S. D. Horkawicz, K. Morris, L. C. Serpell, X. Zuo, J. S. Wall, V. P. Conticello, *J. Am. Chem. Soc.* **2013**, *135*, 15565 – 15578; b) R. K. Kiagus-Armad, A. Brizard, C. Tang, R. Blatchly, B. Desbat, R. Oda, *Chem. Eur. J.* **2011**, *17*, 9999 – 10009; c) R. Tamoto, N. Daugey, T. Buffeteau, B. Kauffmann, M. Takafuji, H. Iharad, R. Oda, *Chem. Commun.* **2015**, DOI: 10.1039/c4cc07972h.

[5] a) A. R. A. Palmans, E. W. Meijer, *Angew. Chem. Int. Ed.* **2007**, *46*, 8948 – 8968; *Angew. Chem.* **2007**, *119*, 9106 – 9126; b) J. S. Park, S. Jeong, D. W. Chang, J. P. Kim, K. Kim, E. K. Park, K. W. Song, *Chem. Commun.* **2011**, *47*, 4736 – 4738; c) F. Rodríguez-Llansola, J. F. Miravet, B. Escuder, *Chem. Commun.* **2009**, 209 – 211; d) J. Makarević, Z. Štefanić, L. Horvat, M. Žinić, *Chem. Commun.* **2012**, *48*, 7407 – 7409**;** e) C. Ou, J. Zhang, X. Zhang, Z. Yang, M. Chen, *Chem. Commun.* **2013**, *49*, 1853 – 1855; f) C. Zhang, J. Wang, J. J. Wang, M. Li, X. L. Yang, H. B. Xu, *Chem. Eur. J.* **2012**, *18*, 14954 – 14956; g) X. Q. Li, V. Stepanenko, Z. Chen, P. Prins, L. D. A. Siebbeles, F. Würthner, *Chem. Commun.* **2006**, 3871 – 3873; h) V. Castelletto, G. Cheng, B. W. Greenland, I. W. Hamley, *Langmuir* **2011**, *27*, 2980 – 2988; i) S. M. Hsu, Y. C. Lin, J. W. Chang, Y. H. Liu, H. C. Lin, *Angew. Chem. Int. Ed.* **2014**, *53*, 1921 – 1927; *Angew. Chem.* **2014**, *126*, 1952 – 1958; j) G. Qing, X. Shan, W. Chen, Z. Lv, P. Xiong, T. Sun, *Angew. Chem. Int. Ed.* **2014**, *53*, 2124 – 2129; *Angew. Chem.* **2014**, *126*, 2156 – 2161; k) H. Hoshizawa, Y. Minemura, K. Yoshikawa, M. Suzuki, K. Hanabusa, *Langmuir* **2013**, *29*, 14666 – 14673; l) N. Yan, Z. Xu, K. K. Diehn, S. R. Raghavan, Y. Fang, R. G. Weiss, *Langmuir* **2013**, *29*, 793 – 805; m) S. J. George, A. Ajayaghosh, P. Jonkheijm, A. P. H. J. Schenning, E. W. Meijer, *Angew. Chem. Int. Ed.* **2004**, *43*, 3422 – 3425; *Angew. Chem.* **2004**, *116*, 3504 – 3507; n) F. Aparicio, L. Sánchez, *Chem. Eur. J.* **2013**, *19*, 10482 – 10486; o) V. Stepanenko, X. Q. Li, J. Gershberg, F. Würthner, *Chem. Eur. J.* **2013**, *19*, 4176 – 4183; p) Y. J. Tian, E. W. Meijer, F. Wang, *Chem. Commun.* **2013**, *49*, 9197 – 9199; q) Z. Qi, C. Wu, P. M. de Molina, H. Sun, A. Schulz, C. Griesinger, M. Gradzielski, R. Haag, M. B. A. Schumacher, C. A. Schalley, *Chem. Eur. J.* **2013**, *19*, 10150 – 10159; r) J. T. van Herpt, M. C. A. Stuart, W. R. Browne, B. L. Feringa, *Chem. Eur. J.* **2014**, *20*, 3077 – 3083; s) F. Aparicio, F. García, L. Sánchez, *Chem. Eur. J.* **2013**, *19*, 3239 – 3248; t) J. Valero, B. Escuder, J. F. Miravet, J. de Mendoza, *Chem. Eur. J.* **2012**, *18*, 13038 – 13047; u) R. Afrasiabi, H. B. Kraatz, *Chem. Eur. J.* **2013**, *19*, 17296 – 17300; v) S. Debnath, S. Roy, R. V. Ulijn, *J. Am. Chem. Soc.* **2013**, *135*, 16789 – 16792.

[6] a) F. M. Menger, A. V. Peresypkin, *J. Am. Chem. Soc.* **2003**, *125*, 5340 – 5345; b) V. S. Balachandran, S. R. Jadhav, P. Pradhan, S. De Carlo, G. John, *Angew. Chem. Int. Ed.* **2010**, *49*, 9509 – 9512; *Angew. Chem.* **2010**, *122*, 9699 – 9702; c) C. B. Minkenberg, W. E. Hendriksen, F. Li, E. Mendes, R. Eelkema, J. H. van Esch, *Chem. Commun.* **2012**, *48*, 9837 – 9839; d) H. Y. Lee, H. Oh, J. H. Lee, S. R. Raghavan, *J. Am. Chem. Soc.* **2012**, *134*, 14375 – 14381; e) S. Himmelein, V. Lewe, M. C. A. Stuart, B. J. Ravoo, *Chem. Sci.* **2014**, *5*, 1054 – 1058.

[7] a) K. J. Skilling, F. Citossi, T. D. Bradshaw, M. Ashford, B. Kellama, M. Marlow, *Soft Matter* **2014**, *10*, 237 – 256; b) E. J. Berns, S. Sur, L. Pan, J. E.

© 2015 Wiley-VCH Verlag GmbH & Co. KGaA, Weinheim

Goldberger, S. Suresh, S. Zhang, J. A. Kessler, S. I. Stupp, *Biomaterials* **2014**, *35*, 185 – 195.

[8] a) M. J. Mayoral, C. Rest, V. Stepanenko, J. Schellheimer, R. Q. Albuquerque, G. Fernández, *J. Am. Chem. Soc.* **2013**, *135*, 2148 – 2151; b) D. E. Fullenkamp, L. He, D. G. Barrett, W. R. Burghardt, P. B. Messersmith, *Macromolecules* **2013**, *46*, 1167 – 1174; c) M. Yan, S. K. P. Velu, M. Maréchal, G. Royal, J. Galveza, P. Terech, *Soft Matter* **2013**, *9*, 4428 – 4436.

[9] a) N. Sreenivasachary, J. M. Lehn, *Chem. Asian J.* **2008**, *3*, 134 – 139; b) D. Dasgupta, S. Srinivasan, C. Rochas, A. Ajayaghosh, J. M. Guenet, *Langmuir* **2009**, *25*, 8593 – 8598; c) A. Saha, B. Roy, A. Garai, A. K. Nandi, *Langmuir* **2009**, *25*, 8457 – 8461; d) B. J. Cafferty, I. Gállego, M. C. Chen, K. I. Farley, R. Eritja, N. V. Hud, *J. Am. Chem. Soc.* **2013**, *135*, 2447 – 2450; e) L. Meazza, J. A. Foster, K. Fucke, P. Metrangolo, G. Resnati, J. W. Steed, *Nat. Chem.* **2013**, *5*, 42 – 47.

[10] a) H. Basit, A. Pal, S. Sen, S. Bhattacharya, *Chem. Eur. J.* **2008**, *14*, 6534 – 6545; b) W. Edwards, D. K. Smith, *J. Am. Chem. Soc.* **2013**, *135*, 5911 – 5920; c) P. Sahoo, R. Sankolli, H. Y. Lee, S. R. Raghavan, P. Dastidar, *Chem. Eur. J.* **2012**, *18*, 8057 – 8063; d) L. Chen, T. O. McDonald, D. J. Adams, *RSC Adv.* **2013**, *3*, 8714 – 8720; e) S. Bhattacharjee, S. Datta, S. Bhattacharya, *Chem. Eur. J.* **2013**, *19*, 16672 – 16681; f) H. Maeda, W. Hane, Y. Bando, Y. Terashima, Y. Haketa, H. Shibaguchi, T. Kawai, M. Naito, K. Takaishi, M. Uchiyama, A. Muranaka, *Chem. Eur. J.* **2013**, *19*, 16263 – 16271; g) P. Wang, J. Hu, S. Yang, B. Song, Q. Wang, *Chem. Asian J.* **2014**, *9*, 2880 – 2884; h) Y. Yoshii, N. Hoshino, T. Takeda, H. Moritomo, J. Kawamata, T. Nakamura, T. Akutagawa, *Chem. Eur. J.* **2014**, *20*, 16279 – 16285; i) Q. Xia, Y. Mao, J. Wu, T. Shu, T. Yi, *J. Mater. Chem. C* **2014**, *2*, 1854 – 1861.

[11] J. Biswas, A. Bajaj, S. Bhattacharya, *J. Phys. Chem. B* **2011**, *115*, 478 – 486.

[12] Y. Liu, T. Wang, Z. Li, M. Liu, *Chem. Commun.* **2013**, *49*, 4767 – 4769.

[13] N. S. S. Kumar, M. D. Gujrati, J. N. Wilson, *Chem. Commun.* **2010**, *46*, 5464 – 5466.

[14] a) X. Yan, D. Xu, X. Chi, J. Chen, S. Dong, X. Ding, Y. Yu, F. Huang, *Adv. Mater.* **2012**, *24*, 362 – 369; b) P. Xing, X. Chu, M. Ma, S. Li, A. Hao, *Chem. Asian J.* **2014**, *9*, 3440 – 3450.

[15] a) E. Krieg, E. Shirman, H. Weissman, E. Shimoni, S. G. Wolf, I. Pinkas, B. Rybtchinski, *J. Am. Chem. Soc.* **2009**, *131*, 14365 – 14373; b) S. Bhattacharjee, S. Bhattacharya, *Chem. Commun.* **2014**, *50*, 11690 – 11693; c) J. Liu, Y. Feng, Z. X. Liu, Z. C. Yan, Y. M. He, C. Y. Liu, Q. H. Fan, *Chem. Asian J.* **2013**, *8*, 572 – 581; d) D. K. Maiti, A. Banerjee, *Chem. Asian J.* **2013**, *8*, 113 – 120; e) A. Dawn, T. Shiraki, S. Haraguchi, S. i. Tamaru, S. Shinkai, *Chem. Asian J.* **2011**, *6*, 266 – 282; f) S. C. Wei, M. Pan, K. Li, S. Wang, J. Zhang, C. Y. Su, *Adv. Mater.* **2014**, *26*, 2072 – 2077; g) T. Tu, W. Fang, Z. Sun, *Adv. Mater.* **2013**, *25*, 5304 – 5313; h) M. Fleischer, C. Schmuck, *Chem. Commun.* **2014**, *50*, 10464 – 10467; i) S. Saha, J. Bachl, T. Kundu, D. D. Diaz, R. Banerjee, *Chem. Commun.* **2014**, *50*, 7032 – 7035; j) P. Xue, J. Sun, Q. Xu, R. Lu, M. Takafuji, H. Ihara, *Org. Biomol. Chem.* **2013**, *11*, 1840 – 1847; k) R. Ochi, T. Nishida, M. Ikeda, I. Hamachi, *J. Mater. Chem. B* **2014**, *2*, 1464 – 1469; l) J. Seo, J. W. Chung, J. E. Kwon, S. Y. Park, *Chem. Sci.*, **2014**, *5*, 4845 – 4850; m) X. Yang, G. Zhang, D. Zhang, *J. Mater. Chem.* **2012**, *22*, 38 – 50.

[16] a) S. Bhattacharjee, S. Bhattacharya, *J. Mater. Chem. A* **2014**, *2*, 17889 – 17898; b) S. Datta, S. K. Samanta, S. Bhattacharya, *Chem. Eur. J.* **2013**, *19*, 11364 – 11373.

[17] a) H. Cui, Z. Chen, S. Zhong, K. L. Wooley, D. J. Pochan, *Science* **2007**, *317*, 647; b) F. He, T. Gädt, I. Manners, M. A. Winnik, *J. Am. Chem. Soc.* **2011**, *133*, 9095 – 9103; c) J. B. Gilroy, T. Gädt, G. R. Whittell, L. Chabanne, J. M. Mitchels, R. M. Richardson, M. A. Winnik, I. Manners, *Nat. Chem.* **2010**, *2*, 566; d) E. Dahan, P. R. Sundararajan, *Langmuir* **2013**, *29*, 8452 – 8458.

[18] a) S. Banerjee, R. K. Das, P. Terech, A. de Geyer, C. Aymonier, A. L. Serani, G. Raffy, U. Maitra, A. D. Guerzo, J. P. Desvergne, *J. Mater. Chem. C* **2013**, *1*, 3305 – 3316; b) E. Elmalem, F. Biedermann, M. R. J. Scherer, A. Koutsioubas, C. Toprakcioglu, G. Biffi, W. T. S. Huck, *Chem. Commun.* **2014**, *50*, 8930 – 8933; c) M. Krogsgaard, A. Andersen, H. Birkedal, *Chem. Commun.* **2014**, *50*, 13278 – 13281; d) H. H. Lee, S. H. Jung, S. Park, K. M. Park, J. H. Jung, *New J. Chem.* **2013**, *37*, 2330 – 2335; e) R. Afrasiabi, H. B. Kraatz, *Chem. Eur. J.* **2013**, *19*, 1769 – 1777; f) X. Du, J. Zhou, B. Xu, *Chem. Asian J.* **2014**, *9*, 1446 – 1472.

Received: October 22, 2014
Published online on ■■ ■■, 0000

© 2015 Wiley-VCH Verlag GmbH & Co. KGaA, Weinheim

FULL PAPER

Gels

*Subham Bhattacharjee, Santanu Bhattacharya**

■■ – ■■

Charge Transfer Induces Formation of Stimuli-Responsive, Chiral, Cohesive Vesicles-on-a-String that Eventually Turn into a Hydrogel

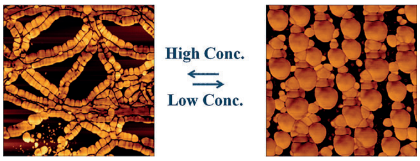

Stringing it along: A charge transfer (CT) mediated two-component supergel shows excellent selectivity in its formation and has a stimuli-responsive nature. The left-handed helical arrangement of the mixed 1:1 CT stacks in the monolayer lipid membranes leads to the formation of chiral interconnected vesicular aggregates with morphological features that resemble "vesicles-on-a-string".

© 2015 Wiley-VCH Verlag GmbH & Co. KGaA, Weinheim

↖↖ These are not the final page numbers!